

PAPER



Cite this: *Dalton Trans.*, 2022, **51**, 580

Diruthenium aryl compounds – tuning of electrochemical responses and solubility†

Lyndsy A. Miller-Clark,  Peter E. Christ and Tong Ren *

Reported herein are the two new series of diruthenium aryl compounds: $\text{Ru}_2(\text{DiMeOap})_4(\text{Ar})$ (**1a–6a**) ($\text{DiMeOap} = 2-(3,5\text{-dimethoxyanilino})\text{pyridinate}$) and $\text{Ru}_2(m\text{-}^i\text{PrOap})_4(\text{Ar})$ (**1b–5b**) ($m\text{-}^i\text{PrOap} = 2-(3\text{-isopropoxyanilino})\text{pyridinate}$), prepared through the lithium-halogen exchange reaction with a variety of aryl halides ($\text{Ar} = \text{C}_6\text{H}_4\text{-4-NMe}_2$ (**1**), $\text{C}_6\text{H}_4\text{-4-}^t\text{Bu}$ (**2**), $\text{C}_6\text{H}_4\text{-4-OMe}$ (**3**), $\text{C}_6\text{H}_3\text{-3,5-(OMe)}_2$ (**4**), $\text{C}_6\text{H}_4\text{-4-CF}_3$ (**5**), C_6H_5 (**6**)). The molecular structures of these compounds were established with X-ray diffraction studies. Additionally, these compounds were characterized using electronic absorption and voltammetric techniques. Compounds **1a–6a** and **1b–5b** are all in the Ru_2^{5+} oxidation state, with a ground state configuration of $\sigma^2\pi^4\delta^2(\pi^*\delta^*)^3$ ($S = 3/2$). Use of the modified ap ligands (ap') resulted in moderate increases of product yield when compared to the unsubstituted $\text{Ru}_2(\text{ap})_4(\text{Ar})$ (ap = 2-anilinopyridinate) series. Comparisons of the electrochemical properties of **1a–6a** and **1b–5b** against the $\text{Ru}_2(\text{ap}')\text{Cl}$ starting material reveals the addition of the aryl ligand cathodically shifted the $\text{Ru}_2^{6+/5+}$ oxidation and $\text{Ru}_2^{5+/4+}$ reduction potentials. These oxidation and reductions potentials are also strongly dependent on the *p*-substituent of the axial aryl ligands.

Received 22nd November 2021,
Accepted 9th December 2021

DOI: 10.1039/d1dt03957a

rs.c.li/dalton

Introduction

Chemistry of diruthenium paddlewheel compounds has prospered since the discovery and structural characterization of diruthenium(II,III) tetracarboxylates by the groups of Wilkinson¹ and Cotton,² respectively. Besides carboxylates, a variety of *N,O*- and *N,N'*-bridging bidentate ligands have been employed to support diruthenium paddlewheel motifs.^{3,4} Among the distinctive features of diruthenium compounds are the rich redox characteristics and a remarkable range of accessible oxidation states from $\text{Ru}_2(\text{I,II})$ to $\text{Ru}_2(\text{III,IV})$, which have been detailed in a comprehensive review by Kadish and co-workers.⁵ The closeness of the π^* and δ^* orbital energies in these compounds has resulted in interesting magnetic properties, and potential molecular magnets based on 1D, 2D and 3D extended structures have been explored by the groups of Handa^{6,7} and Miller.^{8,9} Diruthenium compounds supported by carboxylates, carbonates, and amidates are also capable of catalyzing homogeneous oxidation reactions.^{10–15}

In the realm of diruthenium organometallic compounds, alkynylation reactions were first explored by the groups of Cotton,¹⁶ and Bear and Kadish,^{17–19} basing on $\text{Ru}_2(\text{ap})_4$ build-

ing block (ap = 2-anilinopyridinate). Inspired by these pioneering efforts, our laboratory has extensively explored both mono- and bis-alkynyl diruthenium compounds (type **I** in Chart 1) with three classes of bridging ligands, DARF (*N,N'*-diarylformamidinate), ap and DMBA (*N,N'*-dimethylbenzamidinate).^{20,21} The aforementioned rich and robust redox chemistry has rendered these Ru_2 alkynyl compounds, primarily ap based, ideal candidates for the investigation of electron delocalization across oligoyn-diyls,^{22–25} and fabrication of molecular wires and devices.^{26–29} Groups of Lehn,³⁰ Kuhn,³¹ Peng,³² and Zuo³³ also explored the chemistry of Ru_2 alkynyl compounds with outcomes complementary to ours. Most recently, Akita and co-workers demonstrated the enhancement of molecular conductance through proper alignment between the HOMO energy of *trans*- $\text{Ru}_2(\text{DARF})_4(\text{C}_2\text{Ar})_2$ species and the Fermi level of metal electrode.³⁴ In parallel to alkynylation, our laboratory recently demonstrated that both $\text{Ru}_2(\text{ap})_4\text{Cl}$ and $\text{Ru}_2(\text{DMBA})_4\text{Cl}_2$ undergo arylation reactions when treated with LiAr to afford

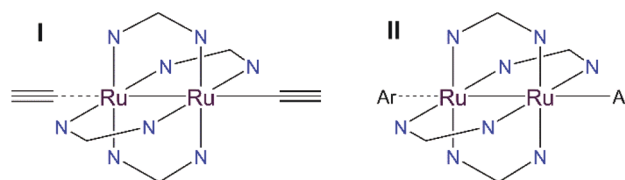


Chart 1 Diruthenium alkynyl and aryl compounds.

Department of Chemistry, Purdue University, West Lafayette, Indiana 4790, USA.

E-mail: tren@purdue.edu

† Electronic supplementary information (ESI) available. CCDC 2123249–2123256. For ESI and crystallographic data in CIF or other electronic format see DOI: 10.1039/d1dt03957a

$\text{Ru}_2(\text{ap})_4(\text{Ar})^{35}$ and $\text{Ru}_2(\text{DMBA})_4(\text{Ar})_2$,³⁶ respectively (type **II** in Chart 1). $\text{Ru}_2(\text{ap})_4(\text{Ar})$ undergoes further reactions with small molecules (Z), namely CN^- , C_2H^- and CO, at the vacant axial site to afford $[\text{Z-Ru}_2(\text{ap})_4(\text{Ar})]$ products that are diverse in electronic and magnetic properties.³⁷ The only other known aryl/alkyl species based on the bimetallic paddlewheel motif are bis(phenyl)dirhodium(III) species reported by Doyle and co-workers,^{38–41} and $\text{Rh}_2(\text{ap})_4(\text{Ph})$ and $\text{Rh}_2(\text{ap})_4(\text{Me})$ by Bear and Kadish.⁴² Both the paucity of bimetallic aryl compounds and interesting physical properties unveiled for $\text{Ru}_2(\text{ap})_4(\text{Ar})$ and $\text{Ru}_2(\text{DMBA})_4(\text{Ar})_2$ warrant further investigation of Ru_2 -aryl chemistry. Aiming at the improvement of organic solubility, we have explored the arylation reactions of $\text{Ru}_2(\text{ap}')_4\text{Cl}$ ($\text{ap}' = 2$ -(3-iso-propoxyanilino)pyridinate (m - PrOap) and 2-(3,5-dimethoxyanilino)pyridinate (DiMeOap)), and the details are reported here.

Experimental

General methods

$\text{Ru}_2(\text{DiMeOap})_4\text{Cl}^{43}$ and $\text{Ru}_2(m\text{-PrOap})_4\text{Cl}^{44}$ were prepared using literature methods. $n\text{-BuLi}$ (2.5 M in hexanes) was purchased from Sigma-Aldrich. All other halogenated ligands were purchased from commercial vendors and used without further purification. Tetrahydrofuran (THF) was freshly distilled over sodium/benzophenone. All reactions were performed under a dry nitrogen atmosphere implementing standard Schlenk procedures unless otherwise noted, with workups occurring in ambient conditions. The syntheses of **1a–6a** and **1b–5b** were performed using modified literature procedures.³⁵ Synthetic examples with each type of $\text{Ru}_2(\text{ap}')_4\text{Cl}$ starting material are provided below, while the rest are described in the ESI.†

Physical methods

UV-vis-NIR spectra were obtained with a JASCO V-670 spectrophotometer in THF solutions. ESI-MS were analyzed on an Advion Mass Spectrometer. ^1H NMR spectra were recorded on a Varian Inova 300 spectrometer operating at 300 MHz. Effective magnetic moments (at 20–22 °C) were obtained using the Evans method⁴⁵ with ferrocene as the standard. Cyclic and differential pulse voltammograms were recorded in 0.1 M ($n\text{-Bu}_4\text{N}$)PF₆ solution (4 mL THF, Ar-degassed) on a CHI620A voltammetric analyzer with a glassy-carbon working electrode (diameter 2 mm), a Pt-wire auxiliary electrode, and a Ag/AgCl reference electrode. The concentration of Ru_2 species was always ca. 1.0 mM. Elemental analyses were performed by Atlantic Microlab, Inc. Single crystal X-ray diffraction data were collected on Nonius Kappa CCD and Bruker Quest Instruments as detailed in the ESI.†

Synthesis

$\text{Ru}_2(\text{DiMeOap})_4(\text{C}_6\text{H}_4\text{-4-}^t\text{Bu})$ (2a). 1-Bromo-4-(*tert*-butyl)-benzene (0.20 mL, 1.2 mmol) was dissolved in 5 mL THF and was treated with 0.60 mL $n\text{-BuLi}$ (1.5 mmol) at 0 °C. The aryllithium solution was then cannula-transferred to a 30 mL solution of $\text{Ru}_2(\text{DiMeOap})_4\text{Cl}$ in THF (125 mg, 0.11 mmol). A color change from green to red-brown was observed. The reaction

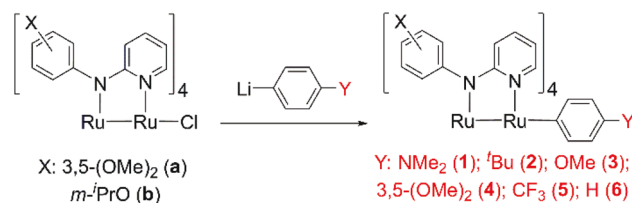
stirred for 1 h and upon exposure to air the color of the solution changed back to dark green. After filtering over Celite and removal of the solvent, the crude product mixture was purified by column chromatography on deactivated (with triethylamine) silica. The dark green band was eluted with 1 : 1 THF/hexanes (v/v), and a dark green solid was isolated from the filtrate. Single crystals suitable for X-ray diffraction were grown by layering hexanes over a concentrated solution of **2a** in EtOAc. Yield: 102 mg (75% based on Ru). Elem. Anal. Found (calcd) for $\text{C}_{76}\text{H}_{95}\text{N}_8\text{O}_{10}\text{Ru}_2$ (**2a**·1.5THF·1C₆H₁₄): C, 61.95 (61.44); H, 6.14 (6.34); N, 7.58 (7.75). ESI-MS (m/z , based on ^{101}Ru): $[\text{M} + \text{H}]^+ = 1253.9$. UV-Vis (in THF) λ/nm ($\epsilon/\text{M}^{-1}\text{cm}^{-1}$): 472 (7000), 642 (1700), 834 (3500). μ_{eff} (21 °C) = $3.9\mu_{\text{B}}$. Electrochemistry (THF, vs. $\text{Fc}^{+/0}$) $E_{1/2}/\text{V}$, $\Delta E_{\text{p}}/\text{mV}$, $i_{\text{backward}}/i_{\text{forward}}$: −0.20, 65, 0.96; −1.60, 71, 0.96.

$\text{Ru}_2(m\text{-PrOap})_4(\text{C}_6\text{H}_4\text{-4-}^t\text{Bu})$ (2b). 1-Bromo-4-(*tert*-butyl)-benzene (0.10 mL, 0.87 mmol) was dissolved in 5 mL THF and treated with 0.50 mL $n\text{-BuLi}$ (1.3 mmol) at 0 °C. The aryllithium solution was cannula-transferred to a 70 mL THF solution of $\text{Ru}_2(m\text{-PrOap})_4\text{Cl}$ (100 mg, 0.087 mmol). An immediate color change from dark green to red-brown was observed. The reaction mixture stirred for 3 h at room temperature. Upon exposure to air, the solution changed from red-brown to dark green. After filtration over Celite and removal of solvent, the crude reaction mixture was purified *via* recrystallization from *n*-pentane at −20 °C. The microcrystalline green precipitate was collected on a frit and rinsed with cold pentane, then dried under vacuum. Compound was later purified for EA using column chromatography on deactivated (w/triethylamine) silica. The dark green band was eluted with 1 : 5 EtOAc/hexanes (v/v) from which a dark green solid was isolated. Single crystals suitable for X-ray diffraction were grown from slow evaporation of **2b** in hexanes. Yield: 84 mg (78% based on Ru). Elem. Anal. Found (calcd) for $\text{C}_{80}\text{H}_{103}\text{N}_8\text{O}_8\text{Ru}_2$ (**2b**·1C₆H₁₄·2EtOAc): C 64.14 (63.77); H 6.93 (6.89); N 7.16 (7.44). ESI-MS (m/z , based on ^{101}Ru): $[\text{M}]^+ = 1244.2$. UV-Vis (in THF) λ/nm ($\epsilon/\text{M}^{-1}\text{cm}^{-1}$): 470 (7500), 650 (2000), 817 (3700). μ_{eff} (20 °C) = $4.1\mu_{\text{B}}$. Electrochemistry (THF, vs. $\text{Fc}^{+/0}$) $E_{1/2}/\text{V}$, $\Delta E_{\text{p}}/\text{mV}$, $i_{\text{backward}}/i_{\text{forward}}$: −0.21, 69, 0.91; −1.61, 76, 0.90.

Results and discussion

Synthesis

As shown in Scheme 1, the reaction between $\text{Ru}_2(\text{ap}')_4\text{Cl}$ and LiAr resulted in the generation of $\text{Ru}_2(\text{ap}')_4(\text{Ar})$ and LiCl. These



Scheme 1 Conditions: 6–10 equiv. LiAr, THF, room temperature, N₂, 1–3 h.

reactions were usually complete within 2 h and the completion is accompanied with easily identifiable color changes. The $\text{Ru}_2(\text{DiMeOap})_4(\text{Ar})$ series was isolated in with either purification over deactivated silica or simple recrystallization with yields ranging from 28–91%. Meanwhile, purification of the $\text{Ru}_2(m^i\text{PrOap})_4(\text{Ar})$ compounds were only successfully using Et_3N deactivated silica in yields ranging between 21–68%. While both ap' series exhibited improved solubility in non-polar organic solvents compared to the ap series (see Table S4† for solubility comparison), the higher yields and easier purification for compounds **1a–6a** points to the advantage of the DiMeOap ligand over the $m^i\text{PrOap}$ ligand.⁴⁴

While **3a/b** undergo partial degradation over the course of a week resulting in low yields (**3a**: 28% and **3b**: 21%), all other reported aryl compounds are stable in ambient conditions as both solutions and solids over a month. The effective magnetic moments (Evans method) for both $\text{Ru}_2(\text{DiMeOap})_4(\text{Ar})$ and $\text{Ru}_2(m^i\text{PrOap})_4(\text{Ar})$ series range from 3.4 to $4.3\mu_{\text{B}}$, all in agreement with an $S = 3/2$ ground state. Compounds **1a–6a** and **1b–5b** were further characterized using mass spectrometry (ESI-MS), electronic absorption spectra, cyclic and differential pulse voltammetry, and single crystal X-ray diffraction studies.

Molecular structures

The structures of compounds **1a**, **2a/b**, **3a/b**, **4a/b** and **5a** were determined with single crystal X-ray diffraction, and those of **1a**, **2a**, **3b**, **4b** and **5a** are shown in Fig. 1–5 with selected bond lengths and angles provided in Table 1. The structural plots of **2b**, **3a** and **4a** are presented in Fig. S1–S3,† and the selected bond lengths and angles are provided in Table S3.† The structures for **2b**, **3b** and **4b** represent the first crystal structures with the modified $m^i\text{PrOap}$ ligand. The bridging ap' ligands adopt the (4,0) arrangement, where all pyridine N-centers coor-

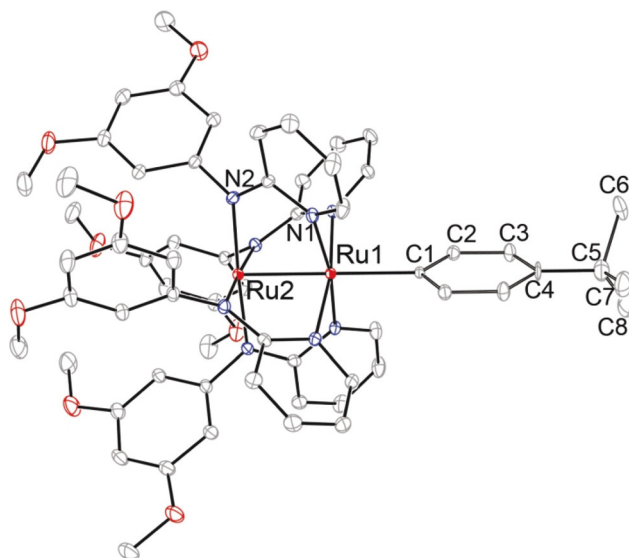


Fig. 2 ORTEP plot of **2a** at 30% probability level. H atoms and $-\text{tBu}$ moiety disorder removed for clarity.

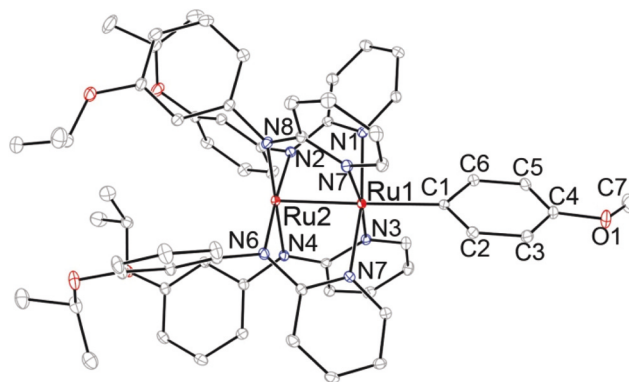


Fig. 3 ORTEP plot of **3b** at 30% probability level. H atoms omitted for clarity.

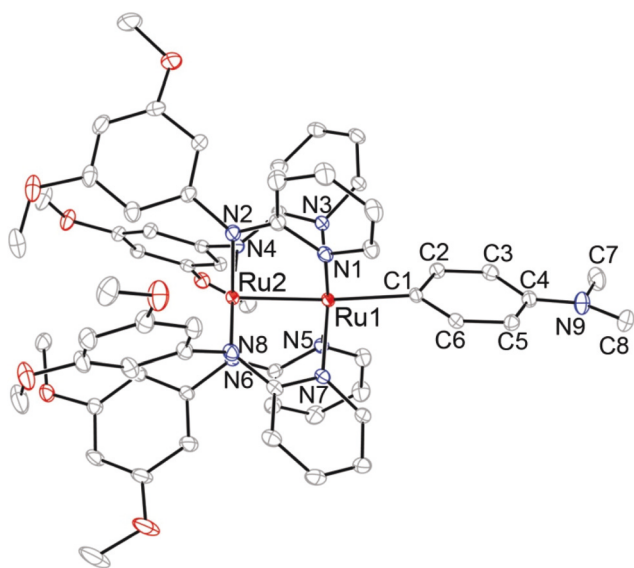


Fig. 1 ORTEP plot of **1a** at 30% probability level. H atoms and solvent molecules removed for clarity.

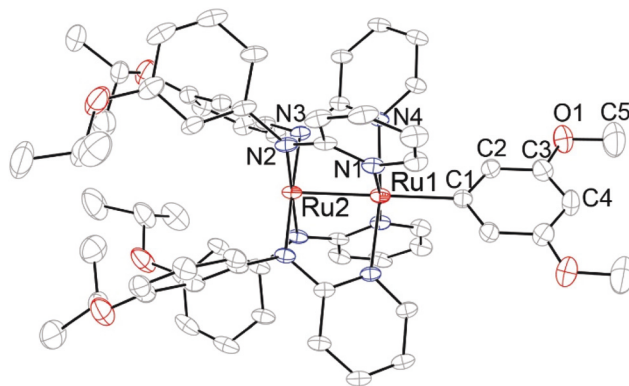


Fig. 4 ORTEP plot of **4b** at 30% probability level. H atoms and solvent molecules omitted for clarity.

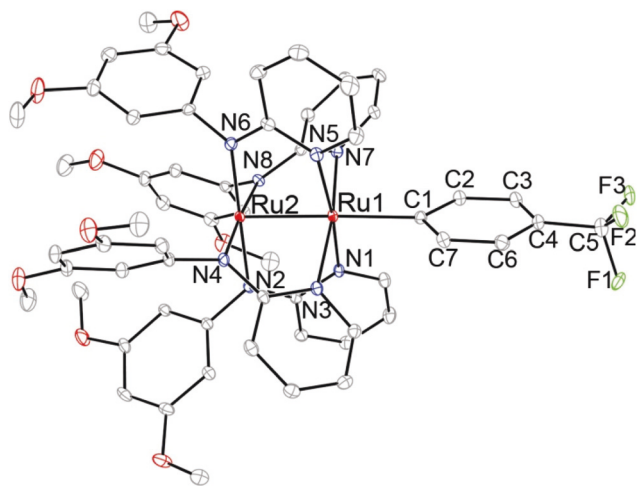


Fig. 5 ORTEP plot of **5a** at 30% probability level. H atoms and $-\text{CF}_3$ moiety disorder omitted for clarity.

Table 1 Selected bond lengths (Å) and angles (°) for compounds **1a**, **2a**, **3b**, **4b** and **5a**

	1a	2a	3b	4b	5a
Ru1–Ru2	2.3414 (2)	2.3277 (4)	2.3326 (2)	2.3467 (8)	2.3341 (3)
Ru1–C1	2.179(2)	2.207(4)	2.187(2)	2.174(6)	2.179(2)
Ru2–Ru1–C1	172.41 (6)	180.0	177.82	180.0	177.38 (6)
Ru1–N1	2.106(2)	2.112(2)	2.102(1)	2.118(3)	2.125(2)
Ru1–N3	2.117(2)	—	2.144(1)	2.119(3)	2.115(2)
Ru1–N5	2.156(2)	—	2.096(1)	—	2.136(2)
Ru1–N7	2.098(2)	—	2.113(1)	—	2.0961 (1)
Ru2–N2	2.035(2)	2.034(2)	2.049(1)	2.033(3)	2.003(2)
Ru2–N4	2.047(2)	—	2.025(1)	2.038(3)	2.041(2)
Ru2–N6	2.020(2)	—	2.049(1)	—	2.022(2)
Ru2–N8	2.044(2)	—	2.027(2)	—	2.041(2)

dinate to the Ru center bonded to Ar, and all anilino N-centers coordinate to the other Ru.²⁰

The Ru–Ru bond lengths for the compounds range from 2.3277(4) (**2a**) to 2.3467(8) (**4b**) Å and are significantly lengthened compared to $\text{Ru}_2(\text{DiMeOap})_4\text{Cl}$ (2.2797(7) Å),⁴³ highlighting the stronger electron-donating nature of the aryl ligand compared to that of the chloro ligand. These Ru–Ru bond lengths have a wider range than those observed in the $\text{Ru}_2(\text{ap})_4(\text{Ar})$ series (2.3370(5) to 2.3423(5) Å),³⁵ demonstrating that modification of the bridging ap' ligands does mildly impact the electronic structure of the Ru_2 core. The Ru–Ru bond lengths in these $\text{Ru}_2(\text{ap}')_4(\text{Ar})$ compounds are also increased when compared to σ -alkynyl compounds $\text{Ru}_2(\text{DiMeOap})_4(\text{C}_{2n}\text{R})$ ($n = 1, 2$), which have Ru–Ru bond lengths of ca. 2.322–2.328 Å.⁴³

The Ru– C_{sp^2} bond lengths for all structures are greater than 2.16 Å, an increase of 0.05–0.10 Å over Ru– C_{sp} bond lengths in the $\text{Ru}_2(\text{DiMeOap})_4(\text{C}_{2n}\text{R})$ type compounds (2.05–2.1 Å).^{22,24,43} While there is a large range in the donicity of aryl substituents,

there is no discernible trend in the Ru– C_{sp^2} bond lengths in both series. Additionally, an intriguing feature of **1a** is the planarity of the $-\text{NMe}_2$ substituent, which was not observed in $\text{Ru}_2(\text{ap})_4\text{-C}_6\text{H}_4\text{-4-NMe}_2$.³⁵ The bond lengths and angles (**1a**: C4–N9–C7 = 119.8(2)°; C4–N9 = 1.390(3) Å; $\text{Ru}_2(\text{ap})_4\text{-C}_6\text{H}_4\text{-4-NMe}_2$: C4–N9–C7 = 116.3(10)°; C4–N9 = 1.408(8) Å) suggest conjugation of the $-\text{NMe}_2$ moiety with the Ru_2 core through the phenylene.

Electronic absorption spectra

The vis-NIR absorption spectra of compounds **1a–6a** and **1b–5b** are shown in Fig. 7 and Fig. S4,† respectively. These compounds are intensely colored, akin to other diruthenium paddlewheel compounds. Like the $\text{Ru}_2(\text{ap})_4(\text{Ar})$ compounds,³⁵ the $\text{Ru}_2(\text{ap}')_4(\text{Ar})$ compounds all display two major electronic transitions (ca. 470 and 800 nm) in the visible region that are characteristic of Ru_2^{5+} compounds. In $\text{Ru}_2(\text{ap})_4\text{Cl}$, the transition at ~470 nm has previously been assigned as $\delta \rightarrow \delta^*$ and the peak at ~800 nm as $\delta \rightarrow \pi^*$.⁴⁶ However, as noted for the $\text{Ru}_2(\text{ap})_4(\text{Ar})$ compounds, spectra for **1a–6a** (Fig. 7) and **1b–5b** (Fig. S4†) exhibit two distinct $\delta \rightarrow \pi^*$ transitions between 600–800 nm. The presence of two transitions was attributed to the removal of the degeneracy of π^* orbitals upon introduction of the aryl ligand based on the DFT study of $\text{Ru}_2(\text{ap})_4(\text{Ar})$.³⁵ This reduces the rotation symmetry about the $\text{Ru}_2(\text{ap}')_4$ core from four-fold (with chloro or mono-alkynyl ligands) to two-fold as demonstrated in Fig. 6 below.

For **1b–5b** these transitions are reminiscent of $\text{Ru}_2(\text{ap})_4(\text{Ar})$, with a small, higher energy shoulder visible. However, this spectroscopic feature is more pronounced in the $\text{Ru}_2(\text{DiMeOap})_4(\text{Ar})$ series (as shown in Fig. 7) where the shoulder present at ca. 650 nm in the $\text{Ru}_2(m\text{-}^i\text{PrOap})_4(\text{Ar})$ (Fig. S4†) and $\text{Ru}_2(\text{ap})_4(\text{Ar})$ ³⁵ series is blue-shifted to approximately 610 nm and has become a distinct transition.

Compounds **1a/b** ($\text{Y} = 4\text{-NMe}_2$) display a unique peak centered at 580 nm, which gives these compounds their unique color (black) compared to the rest of the compounds (green). This unique peak has been assigned with DFT as a high-lying $\pi(\text{Ar}/\text{Ru}_2) \rightarrow \pi^*(\text{Ar}/\text{Ru}_2)$ transition.³⁵ The lack of a corresponding peak in compounds **2a/b** ($\text{Y} = 4\text{-}^t\text{Bu}$) and **3a/b** ($\text{Y} =$

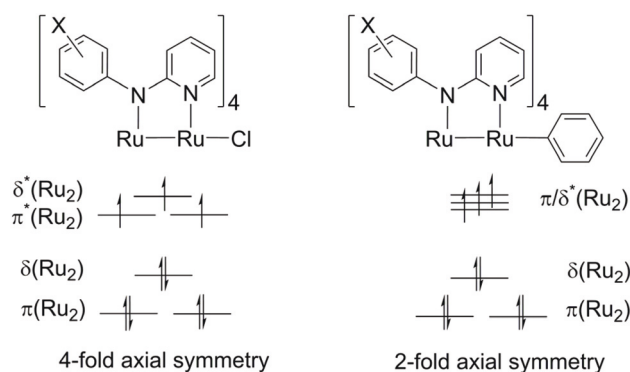


Fig. 6 Qualitative MO diagram of $\text{Ru}_2(\text{ap}')_4$ core upon attachment of aryl ligand (energy levels not drawn to scale).

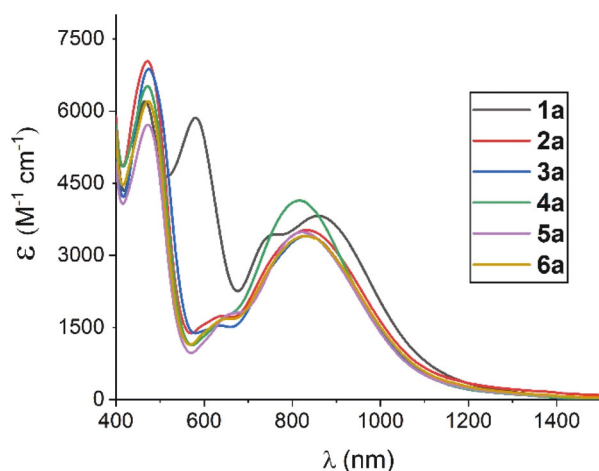


Fig. 7 Vis-NIR absorption spectra of compounds **1a–6a** in THF.

4-OMe) highlights the necessity of a strong electron-donating lone pair on the *para*-substituent to enable this unique transition.

Electrochemical studies

The redox properties of **1a–6a** and **1b–5b** were examined using cyclic (CV) and differential pulse voltammetry (DPV). The voltammograms for **1a–6a** are displayed in Fig. 8 and the electrode potentials given in Table 2, while those for **1b–5b** are in Fig. S5 and Table S5.† All the $\text{Ru}_2(\text{ap}')(\text{Ar})$ species exhibit one reversible oxidation **B** ($\text{Ru}_2^{6+/5+}$) and one reversible reduction **A** ($\text{Ru}_2^{5+/4+}$). Compounds **1a** and **1b** exhibit the second reversible one electron oxidation (**C**), which is attributed to the 4- NMe_2 substituent. Additionally, compound **1b** also displayed the third oxidation at 0.50 V (*versus* Fc, see Fig. S5†), that is likely Ru_2 based ($\text{Ru}_2^{7+/6+}$), analogous to those observed in the $\text{Ru}_2(\text{ap})_4(\text{Ar})$ series.³⁵ Such a wave was not detected in **1a–6a** and **2b–5b** because they are shifted outside the potential window allowed by THF solvent.

The modification to the bridging ligands resulted in slight shifts in electrode potentials between two $\text{Ru}_2(\text{ap}')_4(\text{Ar})$ series, as evidenced in the data for the DMAP ($\text{C}_6\text{H}_4\text{-4-NMe}_2$) derivatives (Table 2). Due to the mild electron withdrawing nature of *meta*-alkoxy group (Hammett constant $\sigma \sim 0.10$), compound **1a** (eight methoxy substituents) is slightly more electron deficient than **1b** (four isopropoxy substituents), and hence its electrode potentials are anodically shifted (70–100 mV) from those of **1b**. Direct comparison between the current $\text{Ru}_2(\text{ap}')_4(\text{Ar})$ series and the original $\text{Ru}_2(\text{ap})_4(\text{Ar})$ series is complicated by the fact that the voltammograms of the latter were recorded in a different solvent (CH_2Cl_2). Further comparison of the $\text{Ru}_2(\text{DiMeOap})_4(\text{Ar})$ series to $\text{Ru}_2(\text{DiMeOap})_4\text{Cl}^{43}$ reveals that the averaged (of compounds **1a–6a**) $E_{1/2}$ ($\text{Ru}_2^{6+/5+}$) and $E_{1/2}(\text{Ru}_2^{5+/4+})$ potentials are cathodically shifted by *ca.* 270 mV and 340 mV, respectively (Table S6†), a testament to the strong donicity of aryl ligands.

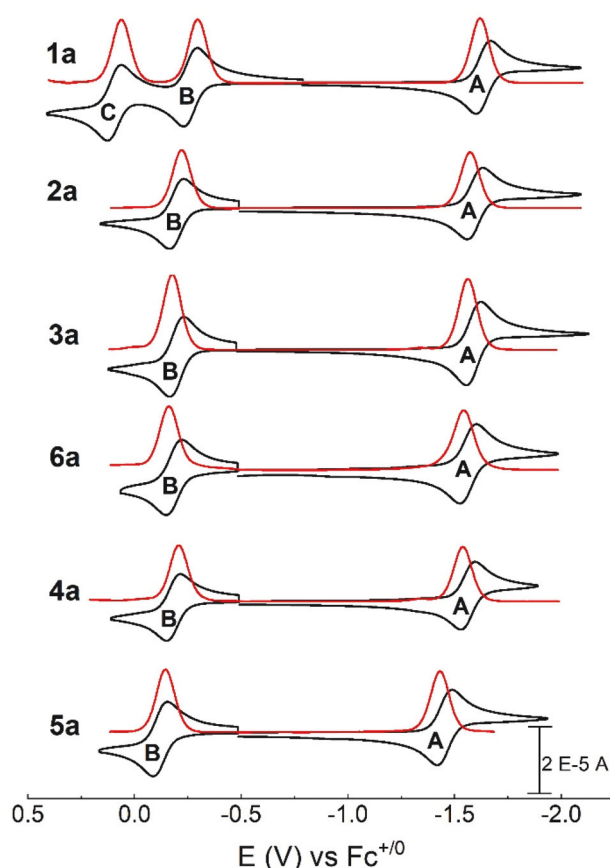


Fig. 8 Cyclic (black) and differential pulse (red) voltammograms of compounds **1a–6a** (1.0 mM) recorded in 0.10 M THF solutions of Bu_4NPF_6 at a scan rate of 0.1 V s^{-1} .

Table 2 Electrochemical data from DPV (in V vs. $\text{Fc}^{+/0}$) for **1a–6a** and other selected compounds

	C	B	A
1a	0.09	−0.26	−1.63
2a	—	−0.20	−1.60
3a	—	−0.20	−1.59
6a	—	−0.18	−1.56
4a	—	−0.18	−1.56
5a	—	−0.12	−1.45
1b	0.00	−0.37	−1.70

As shown in Table 2 and Table S5,† both the reversible reduction (**A**) and oxidation (**B**) potentials for the $\text{Ru}_2(\text{ap}')_4(\text{Ar})$ series vary significantly across each series. These variations depend on the electron donating/withdrawing nature of the aryl *p*-substituent as measured by its Hammett constant (σ_Y). Linear fit plots of the $\text{Ru}_2^{5+/6+}$ oxidation potentials of $\text{Ru}_2(\text{DiMeOap})_4(\text{Ar})$ (Fig. 9) and $\text{Ru}_2(m\text{-}^i\text{PrOap})_4(\text{Ar})$ (Fig. S6†) against the σ_Y of the aryl substituent support this correlation.^{47–49} For $\text{Ru}_2(\text{DiMeOap})_4(\text{Ar})$, a reactivity constant (ρ , the slope of the fit) of *ca.* 93 mV (eqn (1)) was obtained,

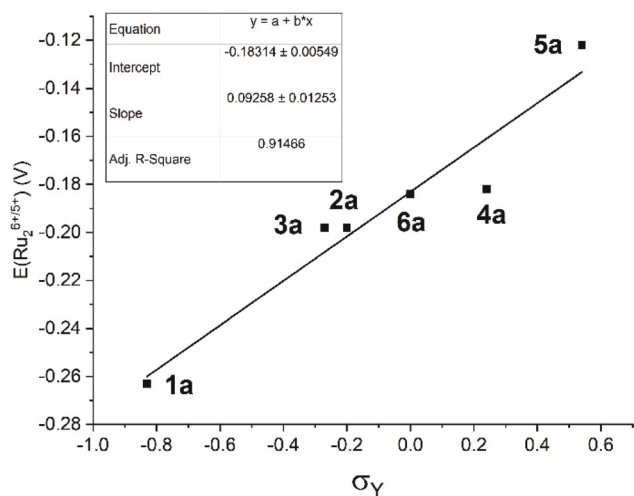


Fig. 9 Hammett plot of **1a–6a** oxidation potentials ($E(\text{Ru}_2^{6+/5+})$) versus σ_Y . The squares are measured oxidation potentials and the solid line is the linear best-fit line.

which matches the ρ obtained from the $\text{Ru}_2(\text{ap})_4(\text{Ar})$ series (*ca.* 98 mV) but is lower than that of $\text{Ru}_2(m\text{-}^i\text{PrOap})_4(\text{Ar})$ ($\rho = 167$ mV).

$$E_{1/2}(X) = \rho\sigma_Y + E_{1/2}(H). \quad (1)$$

The reactivity constants of the reduction couple (**A**) for $\text{Ru}_2(\text{DiMeOap})_4(\text{Ar})$ (134 mV) and $\text{Ru}_2(m\text{-}^i\text{PrOap})_4(\text{Ar})$ (154 mV) agree with each other, but are significantly higher than that of $\text{Ru}_2(\text{ap})_4(\text{Ar})$ (107 mV).³⁵

Conclusions

Reported in this contribution are two new series of $\text{Ru}_2(\text{ap}')_4(\text{Ar})$ compounds with significantly improved solubility in organic solvents (**1a–6a**). All $\text{Ru}_2(\text{ap}')_4(\text{Ar})$ type compounds are of the Ru_2^{5+} oxidation state, and a ground state configuration of $\sigma^2\pi^4\delta^2(\pi^*\delta^*)^3$ ($S = 3/2$). All compounds display at least one reversible oxidation and one reversible reduction, both Ru_2 centered, while those containing an amine functionality (**1a/b**) support a second reversible oxidation. Both the oxidation and reduction electrochemical potentials were tunable through varying the aryl substituent. The much enhanced solubility will enable further exploration of Ru_2 -aryls as both molecular wires and active species in devices similar to the efforts based on Ru_2 -alkynyls,²⁰ which is currently under investigation.

Conflicts of interest

The authors have no conflicts of interest to declare.

Acknowledgements

We gratefully acknowledge financial support from the National Science Foundation (CHE 1764347 and CHE 2102049). PEC thanks the Department of Chemistry of Purdue for an Undergraduate Summer Research Award. The authors wish to dedicate this contribution to the memories of Sir Geoffrey Wilkinson and Al Cotton, the pioneers of diruthenium chemistry.

References

- 1 T. A. Stephenson and G. Wilkinson, *J. Inorg. Nucl. Chem.*, 1966, **28**, 2285–2291.
- 2 M. J. Bennett, K. G. Caulton and F. A. Cotton, *Inorg. Chem.*, 1969, **8**, 1–6.
- 3 P. Angaridis, Ruthenium Compounds, in *Multiple Bonds between Metal Atoms*, ed. F. A. Cotton, C. A. Murillo and R. A. Walton, Springer Science and Business Media, Inc., New York, 2005.
- 4 M. Cortijo, R. González-Prieto, S. Herrero, J. L. Priego and R. Jiménez-Aparicio, *Coord. Chem. Rev.*, 2019, **400**, 213040.
- 5 E. Van Caemelbecke, T. Phan, W. R. Osterloh and K. M. Kadish, *Coord. Chem. Rev.*, 2021, **434**, 213706.
- 6 M. Handa, Y. Sayama, M. Mikuriya, R. Nukada, I. Hiromitsu and K. Kasuga, *Chem. Lett.*, 1996, 201–202.
- 7 M. Handa, Y. Sayama, M. Mikuriya, R. Nukada, I. Hiromitsu and K. Kasuga, *Bull. Chem. Soc. Jpn.*, 1998, **71**, 119–125.
- 8 T. E. Vos, Y. Liao, W. W. Shum, J.-H. Her, P. W. Stephens, W. M. Reiff and J. S. Miller, *J. Am. Chem. Soc.*, 2004, **126**, 11630–11639.
- 9 T. E. Vos and J. S. Miller, *Angew. Chem., Int. Ed.*, 2005, **44**, 2416–2419.
- 10 N. Komiya, T. Nakae, H. Sato and T. Naota, *Chem. Commun.*, 2006, 4829–4831.
- 11 J. E. Barker and T. Ren, *Inorg. Chem.*, 2008, **47**, 2264–2266.
- 12 H. B. Lee and T. Ren, *Inorg. Chim. Acta*, 2009, **362**, 1467–1470.
- 13 M. E. Harvey, D. G. Musaev and J. Du Bois, *J. Am. Chem. Soc.*, 2011, **133**, 17207–17216.
- 14 L. Villalobos, Z. Cao, P. E. Fanwick and T. Ren, *Dalton Trans.*, 2012, **41**, 644–650.
- 15 T. Miyazawa, T. Suzuki, Y. Kumagai, K. Takizawa, T. Kikuchi, S. Kato, A. Onoda, T. Hayashi, Y. Kamei, F. Kamiyama, M. Anada, M. Kojima, T. Yoshino and S. Matsunaga, *Nat. Catal.*, 2020, **3**, 851–858.
- 16 A. R. Chakravarty and F. A. Cotton, *Inorg. Chim. Acta*, 1986, **113**, 19–26.
- 17 J. L. Bear, B. Han and S. Huang, *J. Am. Chem. Soc.*, 1993, **115**, 1175–1177.
- 18 J. L. Bear, B. Han, S. Huang and K. M. Kadish, *Inorg. Chem.*, 1996, **35**, 3012–3021.

- 19 K. M. Kadish, T. D. Phan, L.-L. Wang, L. Giribabu, A. Thuriere, J. Wellhoff, S. Huang, E. V. Caemelbecke and J. L. Bear, *Inorg. Chem.*, 2004, **43**, 4825–4832.
- 20 T. Ren, *Organometallics*, 2005, **24**, 4854–4870.
- 21 T. Ren and G. L. Xu, *Comments Inorg. Chem.*, 2002, **23**, 355–380.
- 22 G. L. Xu, G. Zou, Y. H. Ni, M. C. DeRosa, R. J. Crutchley and T. Ren, *J. Am. Chem. Soc.*, 2003, **125**, 10057–10065.
- 23 G.-L. Xu, R. J. Crutchley, M. C. DeRosa, Q.-J. Pan, H.-X. Zhang, X. Wang and T. Ren, *J. Am. Chem. Soc.*, 2005, **127**, 13354–13363.
- 24 B. Xi, I. P. C. Liu, G.-L. Xu, M. M. R. Choudhuri, M. C. DeRosa, R. J. Crutchley and T. Ren, *J. Am. Chem. Soc.*, 2011, **133**, 15094–15104.
- 25 Z. Cao, B. Xi, D. S. Jodoin, L. Zhang, S. P. Cummings, Y. Gao, S. F. Tyler, P. E. Fanwick, R. J. Crutchley and T. Ren, *J. Am. Chem. Soc.*, 2014, **136**, 12174–12183.
- 26 A. S. Blum, T. Ren, D. A. Parish, S. A. Trammell, M. H. Moore, J. G. Kushmerick, G.-L. Xu, J. R. Deschamps, S. K. Pollack and R. Shashidhar, *J. Am. Chem. Soc.*, 2005, **127**, 10010–10011.
- 27 A. K. Mahapatro, J. Ying, T. Ren and D. B. Janes, *Nano Lett.*, 2008, **8**, 2131–2136.
- 28 H. Zhu, S. J. Pookpanratana, J. E. Bonevich, S. N. Natoli, C. A. Hacker, T. Ren, J. S. Suehle, C. A. Richter and Q. Li, *ACS Appl. Mater. Interfaces*, 2015, **7**, 27306–27313.
- 29 K. Jiang, S. J. Pookpanratana, S. N. Natoli, T. Ren, B. A. Sperling, J. Robertson, C. A. Richter, S. Yu and Q. Li, *Appl. Phys. Lett.*, 2019, **115**, 162102.
- 30 K.-T. Wong, J.-M. Lehn, S.-M. Peng and G.-H. Lee, *Chem. Commun.*, 2000, 2259–2260.
- 31 J.-L. Zuo, E. Herdtweck and F. E. Kuhn, *J. Chem. Soc., Dalton Trans.*, 2002, 1244–1246.
- 32 C. Kuo, J. Chang, C. Yeh, G. Lee, C. Wang and S. Peng, *Dalton Trans.*, 2005, 3696–3701.
- 33 X.-Y. Zhang, Q. Q. Zheng, Q. Chen-Xi and J.-L. Zuo, *Chin. J. Inorg. Chem.*, 2011, **27**, 1451–1464.
- 34 S. Ogawa, S. Chattopadhyay, Y. Tanaka, T. Ohto, T. Tada, H. Tada, S. Fujii, T. Nishino and M. Akita, *Chem. Sci.*, 2021, **12**, 10871–10877.
- 35 A. Raghavan, B. L. Mash and T. Ren, *Inorg. Chem.*, 2019, **58**, 2618–2626.
- 36 A. Raghavan and T. Ren, *Organometallics*, 2019, **38**, 3888–3896.
- 37 A. Raghavan, F. Yuan and T. Ren, *Inorg. Chem.*, 2020, **59**, 8663–8666.
- 38 J. M. Nichols, J. Wolf, P. Zavalij, B. Varughese and M. P. Doyle, *J. Am. Chem. Soc.*, 2007, **129**, 3504–3505.
- 39 J.-H. Xie, L. Zhou, C. Lubek and M. P. Doyle, *Dalton Trans.*, 2009, 2871–2877.
- 40 D. Angelone, A. Draksharapu, W. R. Browne, M. M. R. Choudhuri, R. J. Crutchley, X. Xu, X. Xu and M. P. Doyle, *Inorg. Chim. Acta*, 2015, **424**, 235–240.
- 41 J. Wolf, R. Poli, J.-H. Xie, J. Nichols, B. Xi, P. Zavalij and M. P. Doyle, *Organometallics*, 2008, **27**, 5836–5845.
- 42 J. L. Bear, B. Han, Y. Li, S. Ngubane, E. Van Caemelbecke and K. M. Kadish, *Polyhedron*, 2009, **28**, 1551–1555.
- 43 B. Xi, G. L. Xu, J. Ying, H.-L. Han, A. Cordova and T. Ren, *J. Organomet. Chem.*, 2008, **693**, 1656–1663.
- 44 G. L. Xu, A. Cordova and T. Ren, *J. Cluster Sci.*, 2004, **15**, 413–424.
- 45 D. F. Evans, *J. Chem. Soc.*, 1959, 2003–2005.
- 46 A. R. Corcos, M. D. Roy, M. M. Killian, S. Dillon, T. C. Brunold and J. F. Berry, *Inorg. Chem.*, 2017, **56**, 14662–14670.
- 47 C. Hansch, A. Leo and R. W. Taft, *Chem. Rev.*, 1991, **91**, 165–195.
- 48 S. Dapperheld, E. Steckhan, K. H. G. Brinkhaus and T. Esch, *Chem. Ber.*, 1991, **124**, 2557–2567.
- 49 T. Ren, *Coord. Chem. Rev.*, 1998, **175**, 43–58.